

**Electronic Supporting information**  
**Unexpected benefits of stacking faults on electronic structure and optical emission in wurtzite GaAs/GaInP core/shell nanowires**

Xiaoming Yuan<sup>1,2\*</sup>, Lin Li<sup>1</sup>, Ziyuan Li<sup>2</sup>, Fan Wang<sup>3\*</sup>, Naiyin Wang<sup>2</sup>, Lan Fu<sup>2</sup>, Jun He<sup>1</sup>,

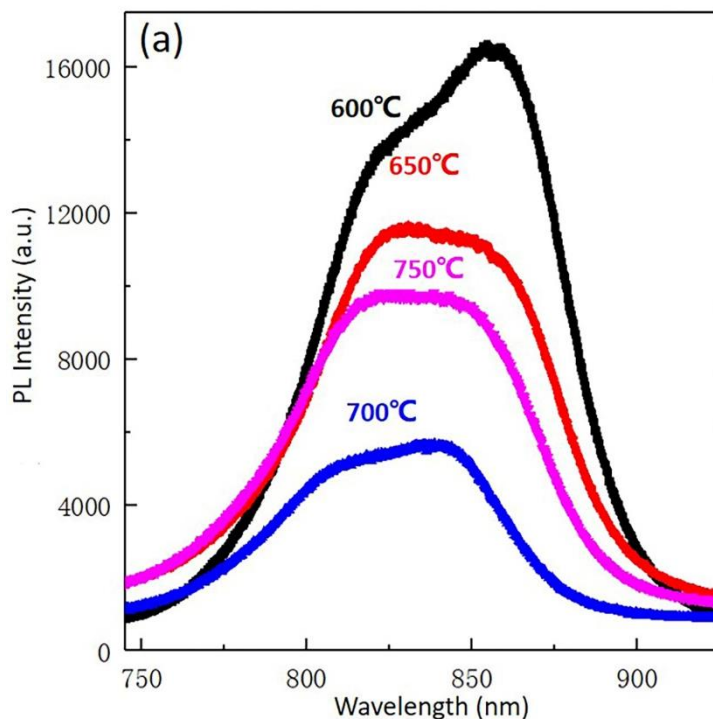
Hark Hoe Tan<sup>2</sup>, Chennupati Jagadish<sup>2</sup>

1. School of Physics and Electronics, Hunan Key Laboratory for Supermicrostructure and Ultrafast Process, Central South University, 932 South Lushan Road, Changsha, Hunan 410083, P. R. China

2. Department of Electronic Materials Engineering, Research School of Physics & Engineering, The Australian National University, Canberra, ACT 2601, Australia.

3. Institute for Biomedical Materials and Devices (IBMD), Faculty of Science, University of Technology Sydney, Sydney, NSW 2007, Australia

\*E-mail: [xiaoming.yuan@csu.edu.cn](mailto:xiaoming.yuan@csu.edu.cn); [fan.wang@uts.edu.au](mailto:fan.wang@uts.edu.au)



sur

Figure S1: (a) PL spectrum of the GaAs/Ga<sub>0.5</sub>In<sub>0.5</sub>P core/shell NWs with shell growth at different temperatures, showing that the shell grown at lower temperature present stronger PL emission. As a consequence, the shell is grown at 600 °C for the GaAs/Ga<sub>0.5</sub>In<sub>0.5</sub>P core/shell NWs discussed in the main texts.

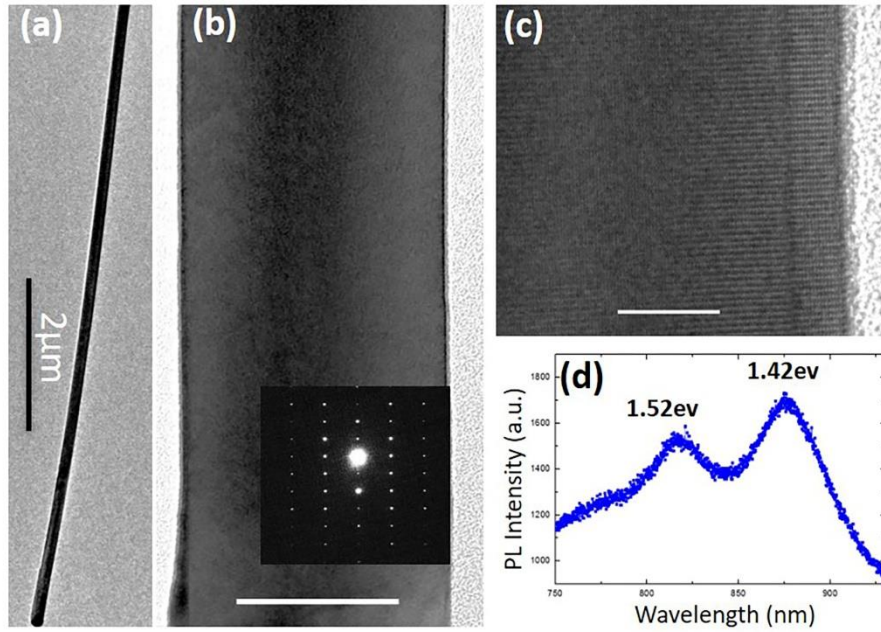


Figure S2: PL emission in a pure WZ GaAs/Ga<sub>0.5</sub>In<sub>0.5</sub>P core/shell NWs. (a-c) bright field TEM images of the selected NW along  $[11\bar{2}0]$  zone axis, showing the pure WZ phase of this NW. Inset in (b) is the corresponding diffraction pattern. (d) Room temperature PL spectrum of this NW, showing the existence of two emission peaks. Since this NW is pure WZ structure, these two peaks thus can only be ascribed to CB-HH and CB-LH transitions. The splitting energy between HH and LH bands is determined to be 100 meV at room temperature. Scale bars in (b) and (c) are 50 nm and 10 nm, respectively.

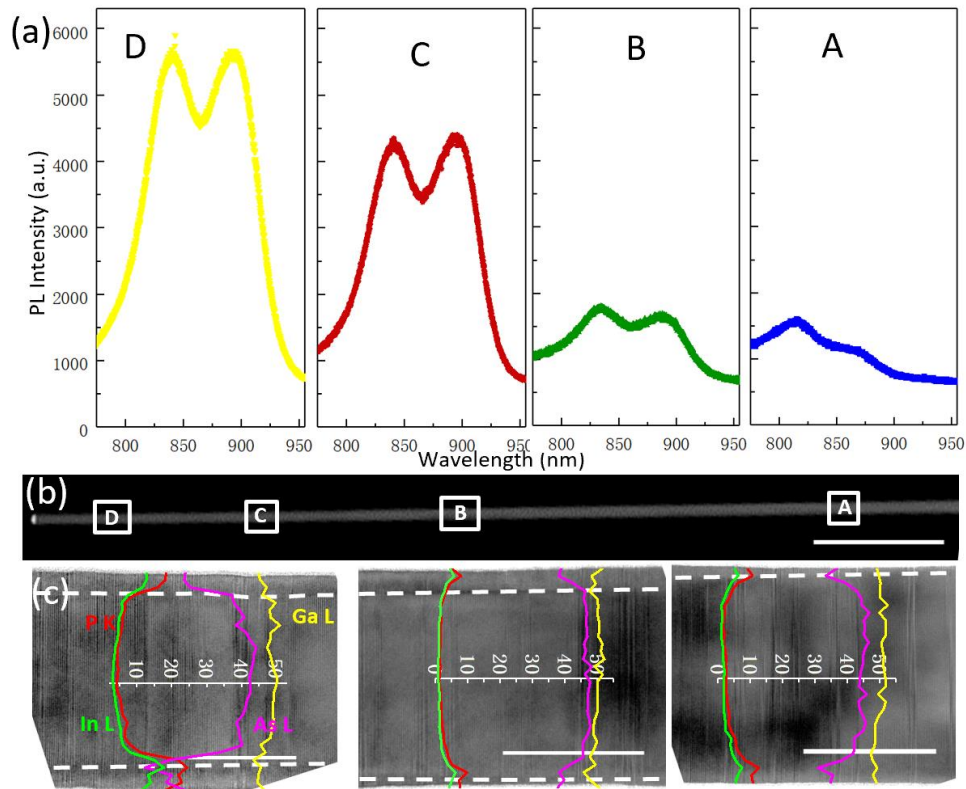


Figure S3 PL and TEM analysis of NW3 with lower emission intensity. (a) PL spectrum at different position of the nanowire in (b), showing the emission intensity increases from the bottom to the top of the nanowire. Moreover, the CB-LH emission intensity is even stronger than the CB-HH transition. (b) HAADF image of the measured nanowire. The marked regions point out the positions where the PL spectra were taken. TEM images along the  $[11\bar{2}0]$  zone axis together with EDX line scan results at tip (c), middle (d) and bottom (e) of the nanowire. TEM and EDX data in Figure 4d-f reveal a much thinner shell than those in Figure 2-3, especially at the bottom of nanowire. The shell coverage becomes more uniform and thicker at the nanowire top, leading to an increased PL emission from bottom to the tip of nanowire. The unit for EDX scan is atom percentage. The scale bars are 1000 nm in (c) and 50 nm in (d-f).

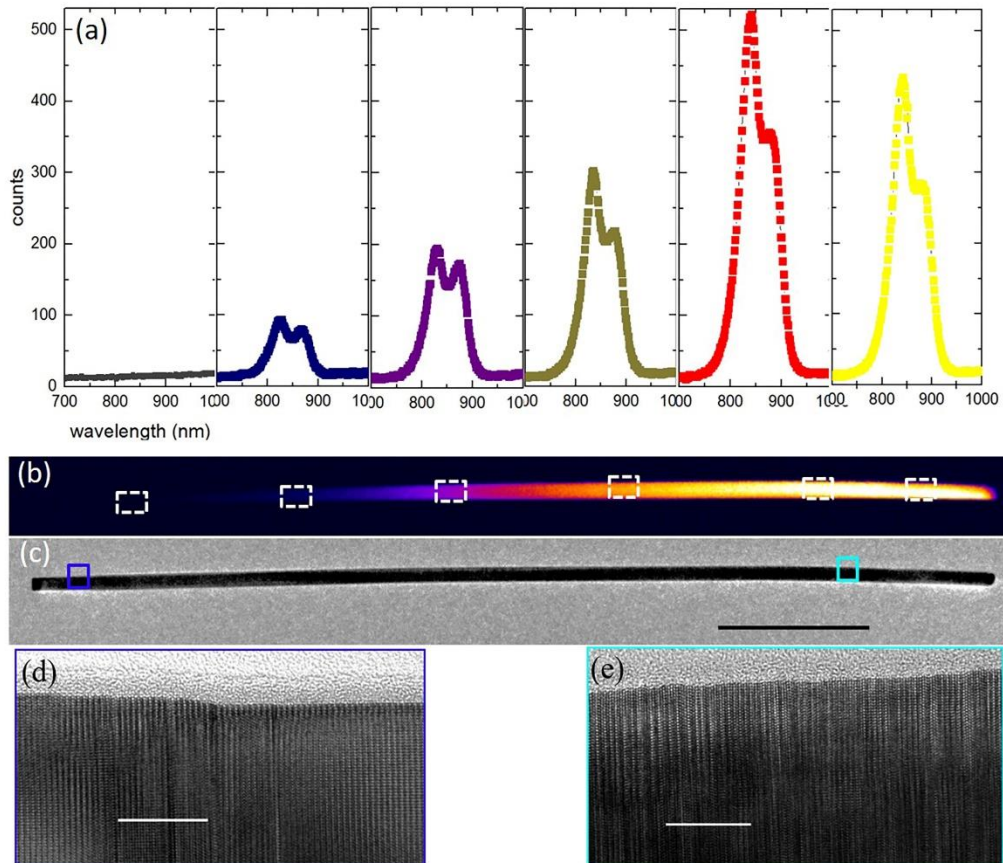


Figure S4 CL and TEM analysis of another nanowire with stronger CB-LH emission. (a) CL spectrum at different position of the nanowire in (b), showing the emission intensity increases from the bottom to the top of the nanowire. Moreover, the CB-LH emission intensity is much stronger than the CB-HH transition. (c) Corresponding TEM image of this nanowire with HRTEM at the base (d) and top (e). The nanowire base mainly consists of pure WZ phase and the shell thickness is much smaller. In contrast, the nanowire top contains a high density of stacking faults with a much thicker GaInP shell. Scale bars in (c-e) are 1  $\mu\text{m}$ , 10 nm and 10 nm, respectively.

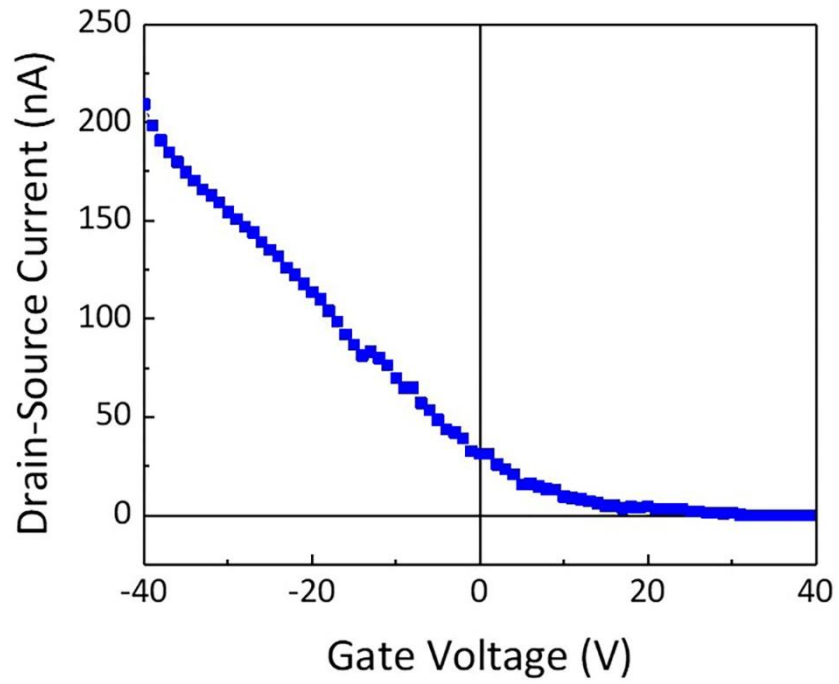


Figure S5: Field effect transistor feature of the NW detector after removing the  $\text{Ga}_{1-x}\text{In}_x\text{P}$  shell layer showing source-drain current versus gate voltage under the source-drain voltage of 1V.